TITLE: Launch Dynamics of the 120-MM M831A1 Heat Training Projectile

LAUNCH DYNAMICS OF THE 120-MM M831A1 HEAT TRAINING PROJECTILE

J. F. Newill,[1] J. Garner,[1] K. Soencksen,[1] and C. P. R. Hoppel[2]

[1] *U.S. Army Research Laboratory, AMSRL-WM-BC, Aberdeen Proving Ground, MD 21005*
[2] *U.S. Army Research Laboratory, AMSRL-WM-MB, Aberdeen Proving Ground, MD 21005*

The M831A1 is the high explosive anti-tank (HEAT) training round used in the 120-mm M256 gun system of the M1 tank. This projectile has been in production for several years and while it typically performs very well, anomalies are occasionally observed. Since this is a training projectile, large numbers are fired each year. As a result, there is constant pressure to reduce the cost of procurement.

In order to understand and improve the performance of the 120-mm M831A1 projectile, a gun-projectile dynamics study was undertaken using the U.S. Army Research Laboratory's (ARL) gun-projectile dynamics simulation codes. The goals of the study were to determine the baseline launch dynamics of the projectile, investigate the performance effects of projectile position in the forcing cone, examine the sealing abilities of the obturator and sealing ring, and examine the effects of worn tubes.

The results show the M831A1's dynamic path differs from its kinetic energy counterpart, the M865, and the general launch state of the projectile. The results also show the projectile's variability at muzzle-exit can be affected by the projectile's initial location in the forcing cone and that the projectile is sensitive to erosion in the M256 gun tube. The sealing ability of the obturator and rubber seal are presented to show that while there are differences in the initial seal, the primary seal is obtained. Finally, an explanation is given for erratic discard of the obturator band.

1.0 INTRODUCTION AND PURPOSE OF THE STUDY

The M831A1 is the high-explosive, anti-tank (HEAT) training round used in the 120-mm M256 gun system of the M1 tank shown in Figure 1. This projectile has been in production for several years and while it typically performs very well, anomalies are occasionally observed. As with all training ammunition, a large number of projectiles are fired, resulting in a constant pressure to minimize projectile procurement costs. Understanding the interactions of the projectile with the gun system and their effect on the subsequent flight provides insight into methods of meeting the goals while maintaining performance.

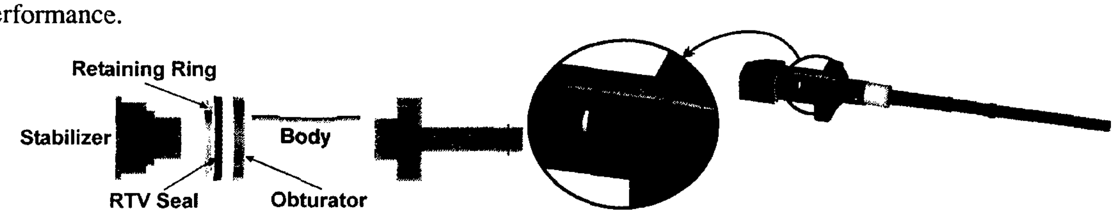

FIGURE 1. PRIMARY COMPONENTS AND A CUT-AWAY VIEWS OF THE M831A1.

The study was initiated by the U.S. Army Armament Research Development and Engineering Center (ARDEC), the Operations Support Command (formerly the Industrial Operations Command), the U.S. Army Research Laboratory (ARL), General Dynamics Ordnance and Tactical Systems (formerly Primex Technologies Inc.) and Alliant Techsystems Inc. The purpose of the study was to describe the in-bore performance of the M831A1 and to show the projectile's sensitivity to system parameters. This paper briefly describes the projectile, along with the modeling techniques, and methods for assessing performance. These descriptions form the groundwork for presenting the basic attributes of launch dynamics, and the effects of launch on the projectile. Focus is then turned to system level performance data to explain the basic behavior along with the factors that influence behavior. Simulation data is compared to ballistic data, with recovered hardware to substantiate the results where possible. The

projectile's obturation system coupled with effects of gun tube erosion are also be presented with hypotheses for the infrequently observed erratic launch. In all over 3,000 simulations were performed

2.0 DESCRIPTION OF THE PROJECTILE AND GUN SYSTEM

The projectile is relatively simple and comprised of six main parts. The nose section is made of steel, while the stabilizer, seal retaining ring, and projectile body are made of aluminum. The seal ring is made of rubber and the obturator is made of Nylon 6. The projectile is full bore in diameter (~119.70 mm [4.712 in]), 476.5 mm (18.76 in) long and weighs is 119.1 N (26.76 lbf).

3.0 SIMULATION TECHNIQUE AND DESCRIPTION OF PERFORMANCE

Gun/projectile dynamic simulations utilize three-dimensional (3-D) Finite Element (FE) models of the M256 120-mm tank cannon launching projectiles. The method is described in Rabern 1991; Wilkerson and Hopkins 1994; Burns, Newill, and Wilkerson (1998); Newill, Burns, Wilkerson (1998); Newill et al. (1998a, 1998b, 1998c, 1999a, 1999b, 2000); Guidos et al. (1999). The hydrocode finite element formulation was chosen to allow investigation of stress wave propagation due to elements of launch. The models are 3-D to capture the asymmetric response of the projectile and gun system resulting from the nonlinear path of the projectile during launch, asymmetric boundary conditions, general lack of symmetry in the centerline profiles of the gun tube, and asymmetric gun motion.

The projectiles and gun systems models are both built in similar manners. Models are developed for the components and then integrated. Relative motion is obtained by defining the proper physics to allow interaction between the parts. Since the M831A1 is relatively simple, the nose, body, stabilizer and obturator are welded together, and sliding interfaces are defined between the nose, body, stabilizer, and the gun bore. One of the purposes of the study is to estimate tank fleet performance. In order to do this, the projectile model is integrated into (and fired from) a number of gun models each of which have unique tube centerlines (the centerlines are covered later in this paper). The propellant pressure loading for the gun system and projectile is generated from IBHVG2 (Anderson and Fickie, 1987).

Projectile performance is often defined in terms of jump, where jump is fully defined in Bornstein et al., 1988; Bornstein, Clemins and Plostins, 1989; Guidos et al. 1999; Soencksen et al. 1999; Soecksen, Newill, and Plostins, 2000 and is also detailed in the previous references to gun dynamic simulations, along with how the jump models have been adapted to the gun dynamic simulations. The gun dynamic simulation codes predict the transverse rates (velocity and angular rate) during the launch cycle. Three types of information are used from these predictions: the dynamic path, variability in jump, and the average jump. The dynamic path gives qualitative information on the rate history of the projectile during the launch cycle. The variability and average jump predicted by the codes are related to accuracy errors where reduction in variability or error represents improved performance of the system. Accuracy error is composed of contributions from many sources, although there are two main contributions from the projectile perspective; dispersion errors, (target impact dispersion TID) and occasion-occasion (occ-occ) error. These concepts are loosely followed in the gun codes i.e., both dispersion and average (center of impact [COI]) are calculated for each group fired, but overall accuracy is not computed in the same manner as in the error budget. The average of a group also has meaning when assessing projectile modifications. If a resulting modification changes the average performance for the projectile, this results in degraded system performance or a potential re-zeroing (new computer correction factor [CCF]) for the projectile.

To intentionally induce the variability into the dynamic path which results in variability the muzzle-exit rates, a series of initial conditions are used, typically the initial cocking angle of the projectile in the forcing cone/bore. Since the diameter of the projectile's bourrelets is less than the interior bore and forcing cone diameter, a clearance exists between the projectile and the gun tube. The angle that the centerline of the projectile can make with these confines is defined as the "cocking angle". There are an infinite number of ways that the projectile can be cocked in tube, but typically, the cocking angles used in

simulations are up, down, left, right, and straight since they encompass the maximum variability. The cocking angles are calculated on a model-by-model basis using the specific dimension of the particular projectile/gun geometry. The straight projectile has the forward and rear bourrelet centered relative to the initial location of the projectile in the gun. Figure 2 defines how the performance envelope is obtained for one projectile, in one gun system, and at one temperature. For a given projectile, when this data is combined with multiple gun systems at a range of temperatures for which tank fleet performance can be defined and then a relative change in performance can be ascertained (Newill et al. to be published).

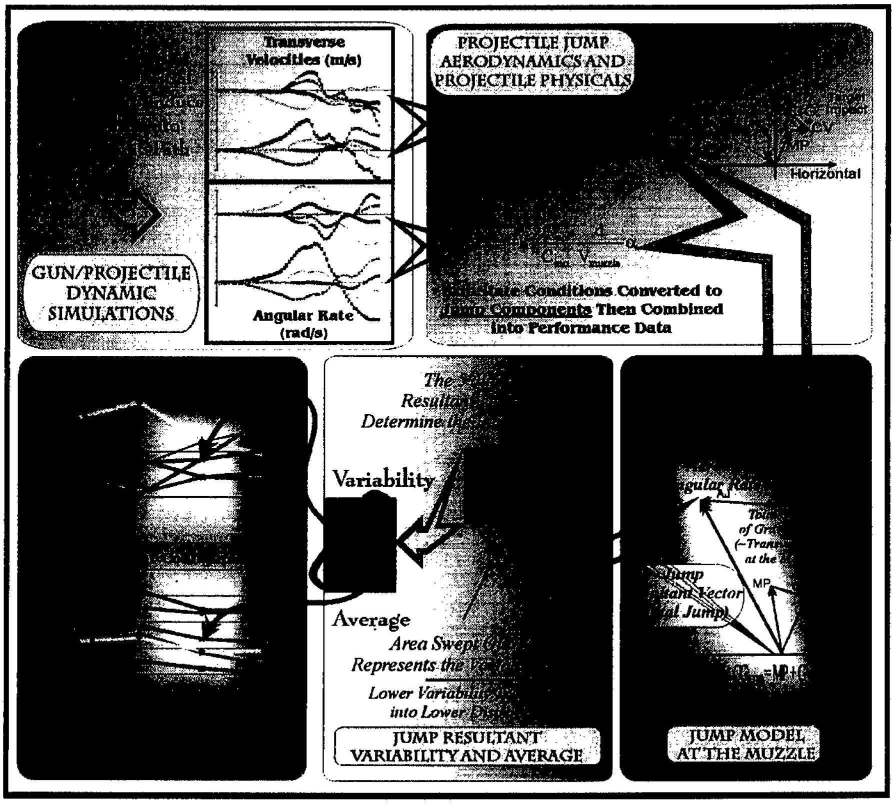

FIGURE 2. DATA ANALYSIS METHODOLOGY.

4.0 LAUNCH DYNAMICS

To understand the launch behavior of the M831A1, the interior ballistic (IB) data is presented first. This data provides an overview of the launch cycle, which pedagogically translates into developing the dynamic path of the M831A1. The dynamic path is compared to that of other ammunition types during the launch cycle. From this basis, system performance of the projectile is addressed.

4.1 Description of the launch event

This study used IBHVG2 (Anderson and Fickie 1987) to approximate the IB loading. The data shows that due to the projectile's relatively heavy mass, it takes approximately 3 ms, or about one third of the launch cycle, to move the projectile the first 0.3 m (12 in) down the gun tube. The projectile travels the remaining 4.32 m (170 in) in approximately 6 ms reaching a nominal velocity of 1,100 m/s and experiencing a peak acceleration of 30 kgees during launch. Figure 3 shows simulation data at several different times, (approximately every 2 ms during launch). Depicted is the effective stress state of the gun along with relative projectile location.

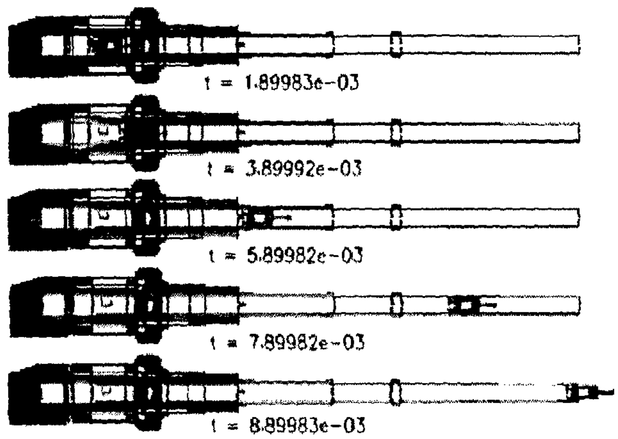

FIGURE 3. EFFECTIVE STRESS STATE AT SEVERAL TIMES.

4.2 Dynamic Path with comparison to other ammunition types

The M831A1 has a relatively long in-bore time, approximately 9 ms, when compared to kinetic energy (KE) projectiles, which are typically approximately about 6 ms. Since the projectile is relatively heavy and stiff, the dynamic path of the projectile would be expected to be very different from its KE counterparts. Figure 4 though Figure 6 shows a comparison in dynamic paths for the M831A1 and a prototype long rod KE projectile, and the M865, a relatively stiff, short wheelbase projectile.

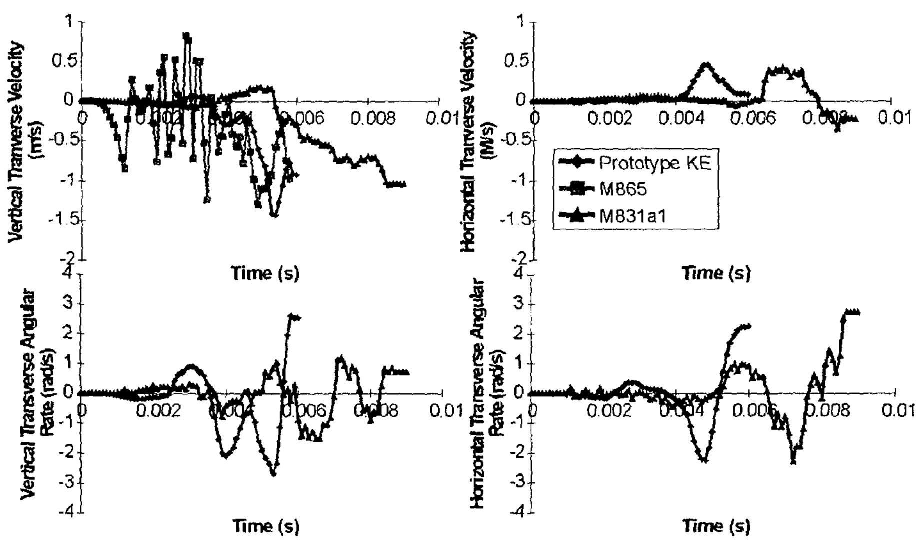

FIGURE 4. COMPARISON OF DYNAMIC PATH WITH PROTOTYPE KE AND THE M865.

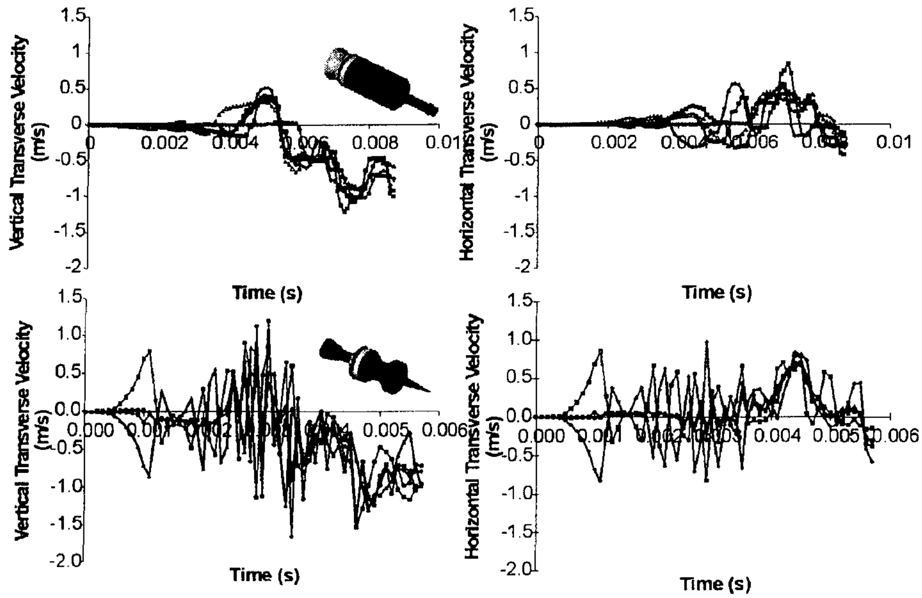

FIGURE 5. COMPARISON OF TRANSVERSE VELOCITY FOR DIFFERENT INITIAL CONDITIONS.

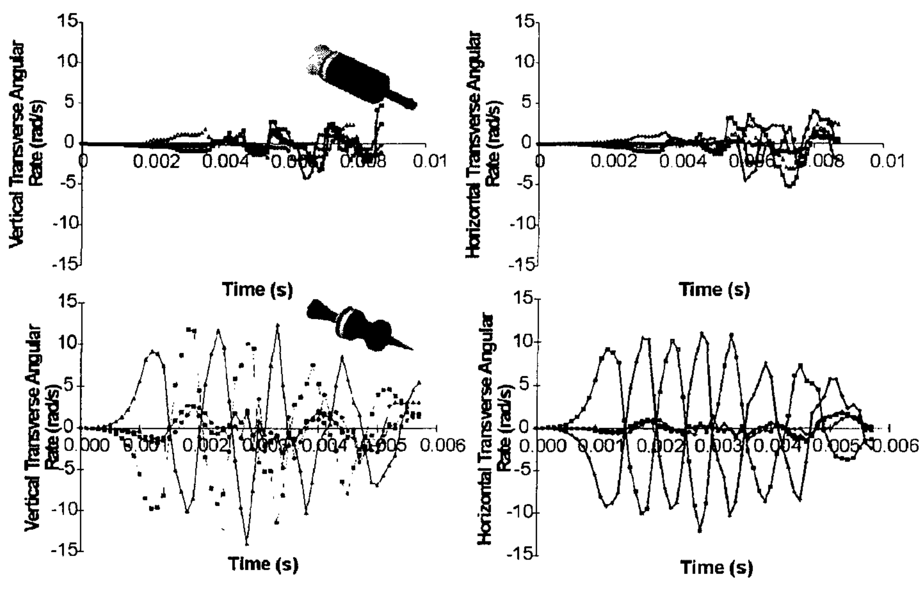

FIGURE 6. COMPARISON OF ANGULAR RATES FOR DIFFERENT INITIAL CONDITIONS.

From the first frame, it is clear that the M865 exhibits a more violent dynamic path than either of the other two projectiles. In the remaining frames, even though the two projectiles (M831A1 and the prototype KE projectile) have very different physical attributes, their in-bore behavior is very similar from a frequency and order of magnitude perspective. While the times are offset due to the velocity differences, the projectile basis response to the system is similar. The reason that the dynamic path for the long rod KE projectile and the M831A1 are probably similar is the relatively low level of balloting experienced during launch. In comparison, the M865's behavior is dominated by balloting probably due to its short wheelbase and small transverse moment of inertia. Again, looking at Figure 4, if the M865 balloting behavior is averaged out, then the projectile follows a path that is similar to the other projectiles.

Figure 5 shows a comparison between transverse velocities and Figure 6 shows a comparison of transverse angular rates velocities of the M865 and the M831A1 for a range of initial conditions. These plots differ from Figure 6 in that the initial conditions have been varied to estimate the relative portion of the total dispersion that will be caused by projectile-gun interaction. From the figures, it is seen that intense balloting behavior does not insure poor performance. It does place more demands on the sealing system of the M865, but the variability is low at muzzle-exit. The M831A1 does not experience the same extreme balloting behavior in-bore, but its variability at muzzle-exit is also relatively low.

These figures illustrate two opposite extremes for a well-designed projectile. Again, if the avg. performance of the M865 is examined instead of the envelope created by the different initial conditions (i.e., removal of balloting), the basic response to the gun system is similar to that of the M831A1.

4.3 Dynamic Effects on the Projectile

The gun system exerts asymmetric loads on the projectile during launch. While the initial conditions of the projectile (cocking angles) are asymmetric with respect to the gun centerline, the initial loading of the projectile is relatively symmetric. Figure 7 shows the effective stress nêar muzzle-exit as well as several earlier times. The stress state in the projectile is clearly asymmetric at this point

The figure shows that the stress state is relatively uniform early in the launch cycle (i.e., 2 ms), but that asymmetries appear by as early as 5 ms, as the projectile starts moving. As the projectile approaches full velocity the stress state is asymmetric.

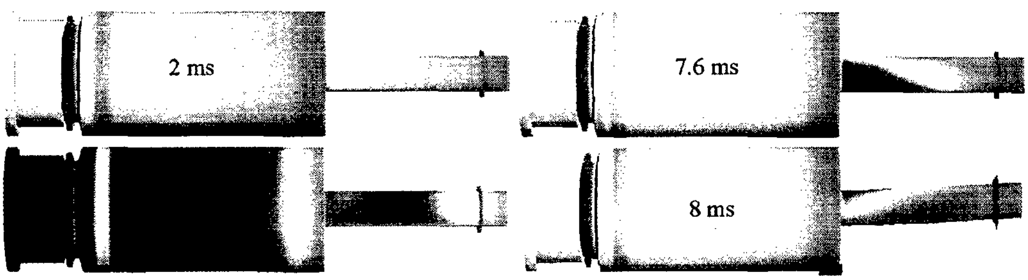

FIGURE 7. EFFECTIVE STRESS STATES AT FOUR TIMES DURING LAUNCH.

4.4 Effect of Initial Projectile Location in the Forcing Cone

Figure 8 shows muzzle-exit jump variability as a function of projectile initial location in the forcing cone. The distance plotted on the x-axis shows the location of the aft point on the rear bourrelet with respect to the rear face of the tube (RFT). The two vertical lines on the graph are significant locations. The first, located at 555 mm (21.85 in), is the furthest aft location of the point on the rear bourrelet that is possible from the tolerance stack up from the drawings. The second line, 565 mm (22.4 in), is the designed, or ideal location of the projectile in the chamber and represents a location at which the obturator is properly engaged. Locations further aft of the 555 mm position represent the point where the back of the rear bourrelet sits outside of the forcing cone although the obturator is still engaged. While these locations lie outside of the total drawing package (TDP), short cartridges in this range have been produced.

Figure 8 shows that the muzzle jump variability is reasonably constant, if the projectile is within the designed tolerances. However, when the initial location of the rear bourrelet starts moving aft of the forcing cone, the variability increases substantially.

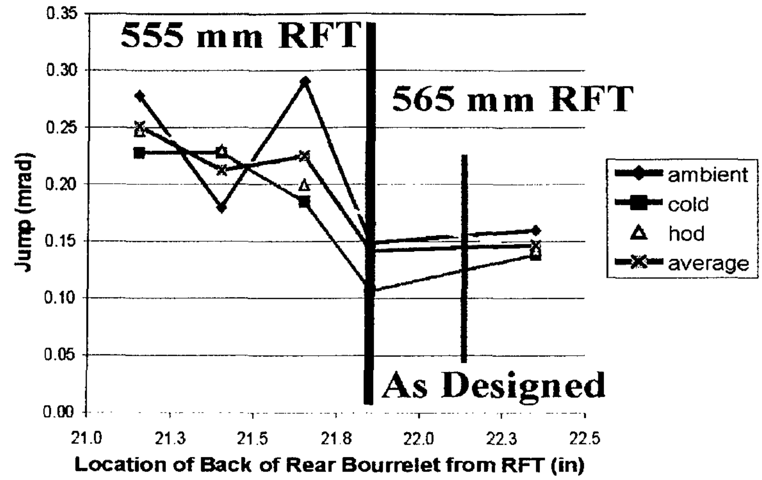

FIGURE 8. MUZZLE JUMP VARIABILITY VS LOCATION OF THE REAR BOURRELET.

There are several other important results from Figure 8. The first is that the source of variability is related to the initial conditions. As the projectile initial location moves aft, the clearance between the forcing cone and the projectile bourrelet increases. The results show that when the projectile is reasonably constrained by the forcing cone, the muzzle variability does not change. Likewise, as the cocking angle is allowed to grow, muzzle variability increases. Therefore, another way to view this figure is the sensitivity of muzzle jump variability to cocking angle. The figure shows that the jump variability grows with increasing cocking angle.

4.5 Centerline Effects and Projectile Jump

Numerous experiments show that the gun tube centerline has a substantial influence on projectile accuracy. Another goal of the present study was to expand the number of gun tube centerlines used to describe tank fleet performance in order to better represent tank fleet performance. Typically, these types of studies have used a "good" tube and a "bad" tube, where the "good" tube conforms to the Held-Wilkerson profile* (uniform profile, tube e). The bad tube's shape is defined as being outside of this profile. Figure 9 shows the centerlines of the ten tubes used in this study.

The gun tube centerline shapes where chosen to represent a range of shapes observed in the tank fleet. The ten shapes encompass the original "good" and "bad" tubes used in the methodology to date. The figures show the tube in the traditional method of supporting the ends of the tubes with gravity removed.

Figure 9 shows the average projectile jump from each of the tubes in the study for three propellant temperatures. In these results, there is a significant deviation in center of impact (COI) with respect to gun tube centerline whereas the temperature effects are less significant. Tube "d" and "e" represent the previous "bad" and "good" centerline tubes, respectively.

* The uniform profile gun tube shape is named after B. Held (formally part of PM-TMAS and current at Rand Corp.) and S. Wilkerson (ARL) for accomplishing the research that identified the importance of this shape.

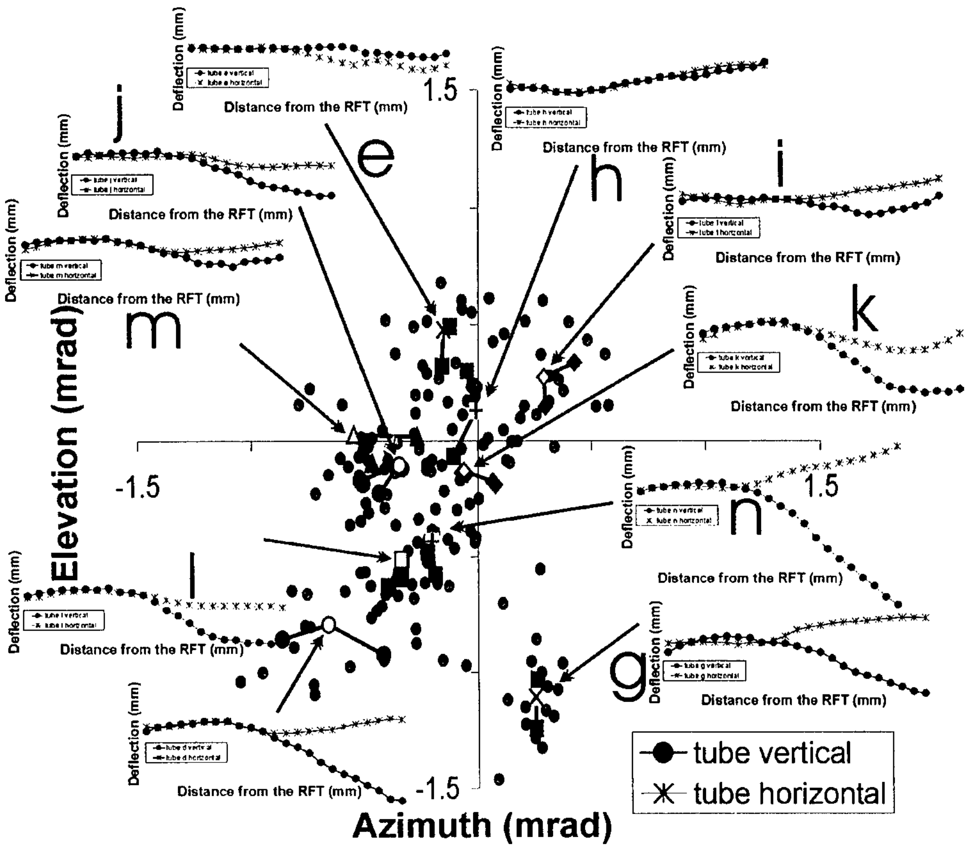

FIGURE 9. AVERAGE JUMP (COI) VERSUS GUN TUBE CENTERLINE.

5.0 COMPARISON WITH EXPERIMENTAL DATA

An experiment was conducted at the Transonic Experimental Facility (TEF) in the Fall of 1998 (Soencksen, Newill, Plostins, 2000, Soencksen et al. 2001) to measure first maximum yaw. The gun tube centerline used in the simulations was that of the actual gun tube used in the TEF experiment. Comparing data to the predicted ranges of first maximum yaw (Soencksen et al. 2001), it is seen that the range and variability are a good match with the exception of one shot. This shot had a first maximum yaw in excess of 9 degrees. Since this very large motion was present immediately in the first yaw cycle, it was necessarily caused by launch disturbances. Inspection of the gun tube at the time of the test showed that the tube had some bore erosion damage . It is confidently hypothesized that the high first maximum yaw for this shot was due to this gun tube damage and would not have been part of the normal population launch from this tube when it was in pristine condition.

In (Soencksen et al. 2001) simulations are used to predict first maximum yaw from a gun tube with bore damage. The envelopes predicted span all the results. It is important to note that simulation of tube damage is extremely difficult due to the complexity of the phenomenon, and no attempt was made to match the exact type of damage seen in the TEF gun tube (beyond the modeling capability). These types of simulations, combined with the experimental data, are used to provide some insight into the sensitivity and the level of performance degradation possible from tube damage.

6.0 OBTURATION

As part of the study, the obturation system of the projectile was examined to help assess its ability to seal the projectile from the propellant gases during launch. It should be noted that the M831A1 discards its obturator band at muzzle-exit in about half of all firings (Manole 1998). Since this behavior represents variability in launch performance, one of the goals of the study was to explain the cause and offer solutions. Table 1 lists the materials properties for Nylon 6 under a range of environmental conditions. The table demonstrates the large range of variability in material that exists in production obturators. This means that the obturator has to function properly almost regardless of its properties.

TABLE 1. NYLON 6 MATERIAL PROPERTIES (DOHRN, 1998).

Condition	# Specimens	Max. Tensile Strength (psi)	Elastic Modulus (ksi)	Elongation to Failure (%)
Brittle	23	11057.9	576	7.75
Tough	12	9569.9	380.87	39.65
Tough-Wet	15	5907.7	23.4	71.62
Variability		2X	25X	9X

Figure 10 shows the configuration of the production projectile. Obturation is achieved through an RTV sealing ring along with a Nylon 6 obturator. One of the first questions addressed was the effectiveness of the sealing ring. Recovered hardware showed areas under the seal containing soot, which indicates gas leakage. The soot deposits were very irregular (asymmetric) with large differences found on each of the recovered projectiles (Demitroff, 1998). There were also signs of soot forward of the sealing ring on the projectile body.

With this information the first step in the modeling was to assess the mechanism of seal gas leakage and to determine if it could prevent the seal from providing adequate protection. Three cases were modeled which are shown in Figure 10.

Even though the three cases represent only an approximation of what is happening to the projectile, in each case the sealing ring offer some level of sealing at relatively early times in the cycle. The reason for this is that the amount of surface area exposed to the gas pressure that contributes positively to the seal is greater than that which contributes negatively.

In these scenarios, it is possible to initially leak gas around the rubber seal and then seal. This is consistent with the recovered hardware. There is no experimental data available on the seal since it does not survive after muzzle-exit , but this is also consistent with gas wash observed on recovered the projectiles.

A similar series of simulations was performed on the nylon obturator, Figure 11. The Nylon 6 was modeled using Bamman plasticity model with constant developed at ARL (Gazonas, 2000). These simulations indicate that the initial sealing pressure is highly dependent on seating locations of the projectile. But even with these initial seating issues, the constriction of the bore forcing cone creates an adequate seal during the ballistic cycle. The figure also shows that the high-compressive-radial stresses occur in the obturator. This correlates well with recovered hardware (Dimitroff, 1998). Relative to the uncertainty of the initial seal, the current obturator design (depending on dimensional factors of the obturator, the body, and location in the forcing cone) can leak propellant gas underneath the band.

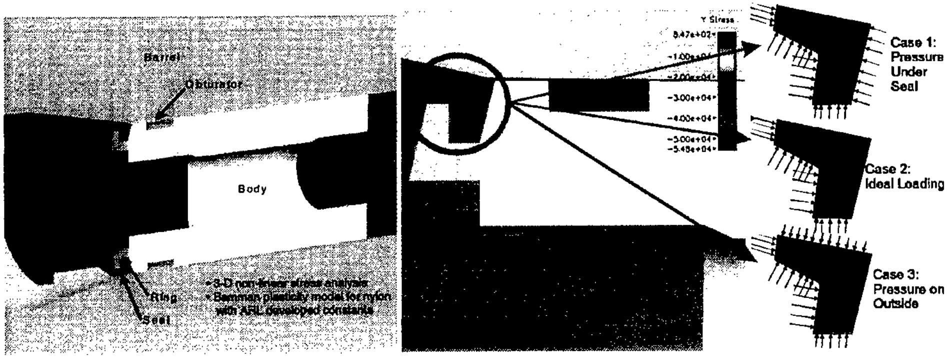

FIGURE 10. CONFIGURATION OF THE SEALS AND BOUNDARY CONDITIONS OF THE MODELS.

Gas leakage underneath the obturator does not degrade the obturator sealing performance, in fact, it increases the sealing efficiency in-bore. The problem occurs at muzzle-exit, where the obturator loses tube support, and the gas either vents or blows the obturator off the projectile body. The sporadic leakage of gas underneath the obturator is believed to be responsible for the intermittent loss of the obturator band at muzzle-exit.

To ensure the bands remain in place, the obturator design was modified to the configuration seen in Figure 12. Figure 13 shows the pressure at the interface of the M831A1 obturator seat. The plot shows the radial sealing pressure at the aft underneath section of the obturator and the sealing pressure under the front of the undercut. For comparison, the negative of the base pressure is plotted. An adequate seal is defined as the absolute value of the obturator-body interface pressure being greater than the absolute value of the base pressure.

The main conclusions from Figure 13 are that a gas seal is present from the beginning of the pressure cycle, and that it continues to increase as peak pressure is approached. The figure also shows that the section underneath the front of the undercut also seals well. Figure 14 also shows a plot at the interface pressure between the obturator and the tube. The graph shows that an adequate seal is created, but not until the projectile moves further into the forcing cone/bore. There actually could be a seal from shot start depending on the initial conditions. If there is an interference fit between the obturator and bore when the cartridge is loaded the initial stress would increase, which could seal the projectile at early times. In either case, the obturator seal the gun gases during launch once the initial seal is formed, it increases at a rate that is faster than the increase in the base pressure. This increasing differential pressure along with the ramp in the obturator seat helps feed the obturator against the bore, and helps maintain sealing as the projectile passes bore damage.

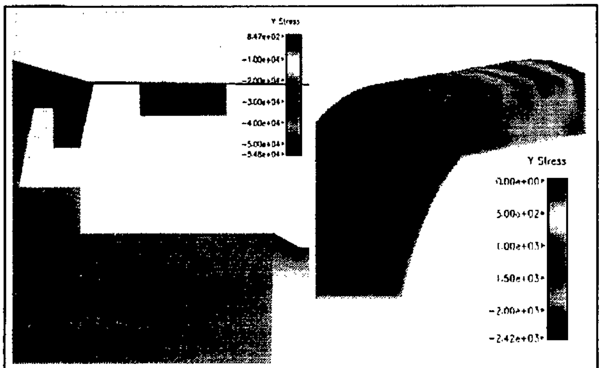

FIGURE 11. OBTURATOR SIMULATION.

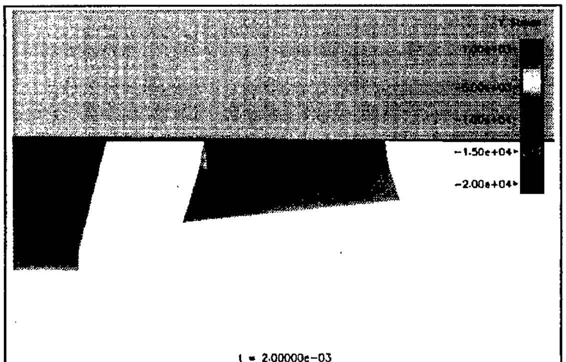

FIGURE 12. RAMP STYLE OBTURATOR.

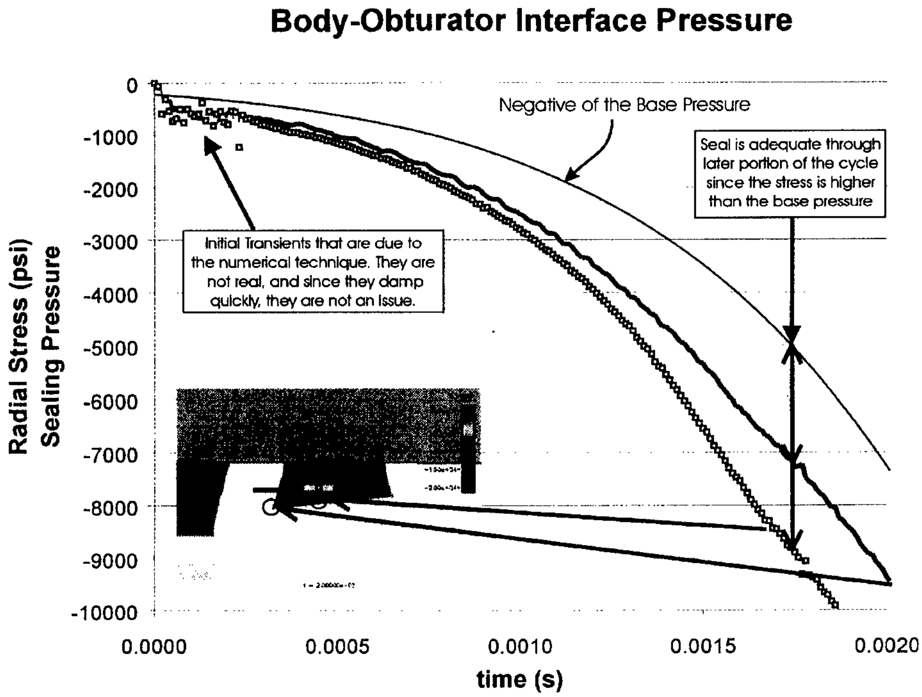

FIGURE 13. M831A1 BODY – OBTURATOR SEAT SEALING.

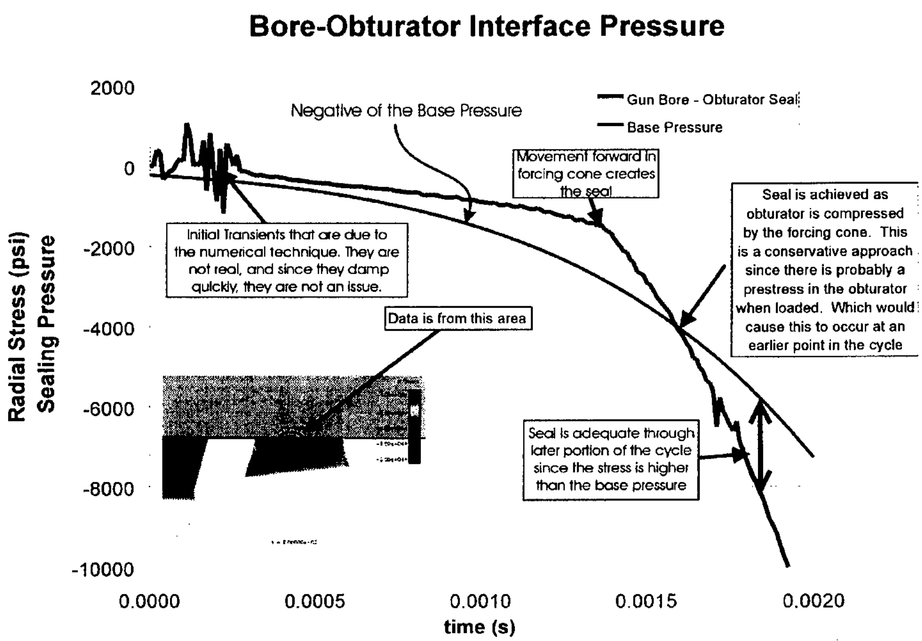

FIGURE 14. M831A1 BODY – BORE SEALING.

7.0 EFFECTS OF GUN TUBE EROSION ON PERFORMANCE

The effect of in-bore damage on projectile performance is very difficult to quantify. It is generally known that as damage to the bore becomes significant it affects system performance through increased projectile dispersion. Even with this knowledge, there is very little research that directly quantifies the phenomenon, since experimental programs rarely use a gun tube with significant bore damage. In general , if control rounds exhibit performance problems and the tube condition is determined to be questionable, the tube is changed. It is also important to note that the type of bore damage of interest here occurs while the gun tube is still considered serviceable, i.e., it is still safe to fire and does not meet condemnation criterion. Since it is likely that tank projectiles will be fired from a gun with some bore damage, this study attempts to address the M831A1 sensitivity to observed types of damage. The remainder of this section briefly quantifies the types of damage of interest and then shows that in some regions of the tube it can affect performance. There are two types of damage that are of primary interest: erosion and chrome stripping. Erosion is typically caused by initial manufacturing defects in the chromed surface of the gun bore that, through repeated firing cycles, cause local damage to the bore surface that continues to erode through the life of the tube (Cote 2000). Figure 15 is a picture of a cast made of the gun tube bore surface with bore erosion damage.

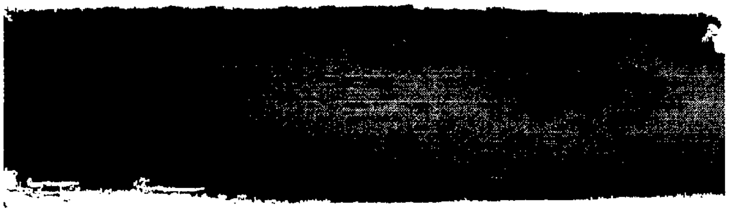

FIGURE 15. TUBE "Y" AFTER 1275 FIRINGS.

The damage seen in Figure 15 consists of long thin (approximately 3 mm wide furrows) regions. These regions are between 50 and 200 mm long, with many that are connect together. Chrome stripping damage is located further down the gun tube and consists of thin strips of chrome removed by the violent mechanical interaction with the projectile. This study takes the approach of trying to assess what types and location of damage affect projectile performance the most.

In order to model this type of damage, many assumptions are made since the interaction between the projectile, obturator, propellant gas, and the damage is extremely complicated. Both the stripping and erosion damage are modeled with respect to leaking gas, but do not include effects caused by the mechanical interaction between the projectile and gun bore. A primary assumption made is that as the projectile and obturator pass gun tube bore damage, local gas jets are opened and closed as the projectile passes the damage (catastrophic failure did not occur). This work does not attempt to quantify the damage to the projectile caused by the jetting, which is recognized in severe cases to cause catastrophic failure. The jet is assumed to cause a localized pressure load on the portion of the projectile forward of the obturator, and this is assumed to ramp up to the base pressure of the projectile for the time it is subjected to the damage, and then drop back down to zero as the projectile passes the damage area. The rise and fall times are assumed approximated to be 0.05 ms.

The duration or size of the modeled damage approximates the types of damage actually seen in the gun tubes. The remainder of this section will first show how the pulses are constructed, then show how size and location could potentially affects the projectile performance.

Figure 16 shows base pressure of the projectile. It also shows that as the projectile passes a particular location with bore damage, the pressure ramps to the base pressure then continues to rise to a pressure between the projectile base pressure and the chamber pressure. Figure 16 also shows the pressure pulses associated with a 1 inch pit at various locations in the gun tube. The reason that the pulses sizes are different is that the projectile's velocity is continually increasing, therefore the dwell time that the pulse has to act on the projectile decreases. At the early times, the length (approximately time of application) of the pulse is relatively long whereas near the muzzle, where the projectile is near full velocity, the pulses' application time are relatively short.

Figure 17 shows a second set of pulses associated with a eight in erosion pit. This figures provides insight into the question of what type of pressure pulse has the greatest influence on the dynamic path of the projectile. Figure 18 shows the pressure impulse (the pressure times the amount of time it is applied. The figure shows that the pressure pulses that impart the most significant energy to the projectile are caused by damage located near the forcing cone of the gun tube. While such early damage has the best chance to impart energy, there is a significant dependence with damage size at locations near the forcing cone.

Both of these effects are related to projectile velocity. If the projectile is moving slowly, then gas leakage has a good chance of significantly impacting the projectile dynamic path. As the velocity increases to a significant level, the projectile passes damage fast enough that the effects of the damage are minimized. Unfortunately the majority of the erosion damage occurs between the chamber and the location of the projectile at peak pressure, which is typically less than 2 m from the RFT.

The first frame of Figure 20 shows the effect of having a 25 to 225 mm erosion pit located 1 m from the RFT and the second frame shows the effect of a 75 mm erosion pit from 0.5 to 4.8 m from the RFT. In both frames, there are three straight horizontal lines near the bottom of the figure. These three lines represent the baseline performance of the projectile at hot (120 F), ambient (70 F), and cold (-20 F) propellant temperatures without any tube damage. The first frame shows results that are chaotic with no

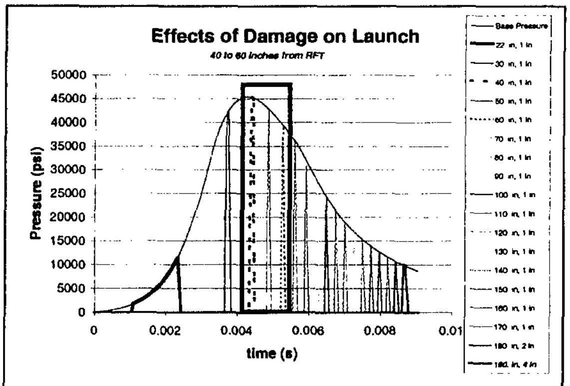

FIGURE 16. PRESSURE PULSES FOR A 1 INCH PITS.

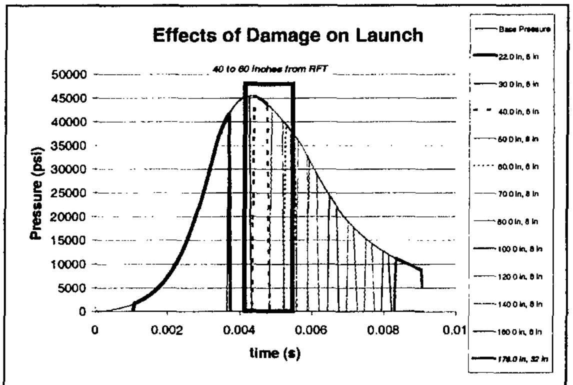

FIGURE 17. PRESSURE PULSES FOR AN 8 INCH PITS.

clear trend with damage size. The figure also shows that in most cases the damage increases the jump variability , but not in all cases although clearly the potential range of exit state conditions has increased. In the second frame the results have a definite trend. As the location of the damage is moved toward the muzzle the damage has less and less effect on the exit state variability.

While in some cases the variability even dropped below the baseline variability, this should not be interpreted as potential method to improve performance, because the overall state is more chaotic which will lead to poorer performance. This study can only give some idea of the sensitivity since it is only examining a single erosion pit or chrome strip that conforms to the assumptions in the study. Figure 20 gives some insight into the effect that more extensive gun damage has on the dynamic path of the projectile. In the case described in the figure random pits were used in gun tube between 0.53 and 2.03 m at various circumferential locations. The figure shows that the dynamic paths were altered significantly and looking at muzzle-exit, the dispersion in the muzzle angular rates has increased substantially. This backs the premise that severe enough damage will substantially alter the launch cycle and degrade the system performance.

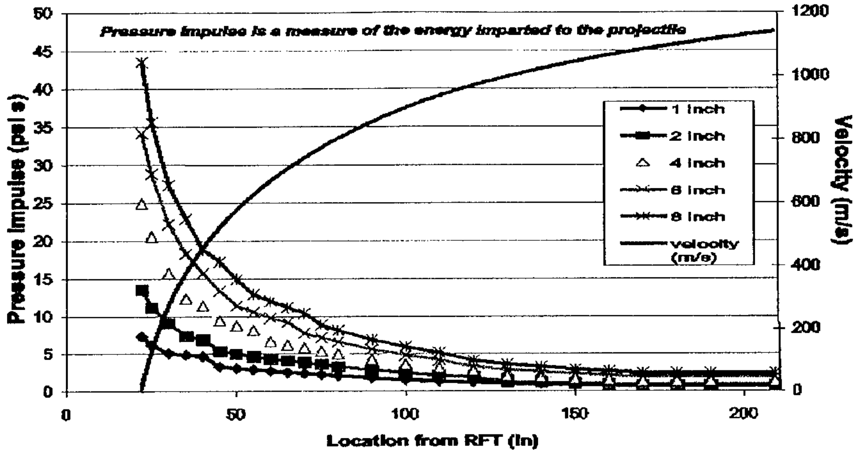

FIGURE 18. PRESSURE IMPULSE VS. DAMAGE SIZE AND LOCATION.

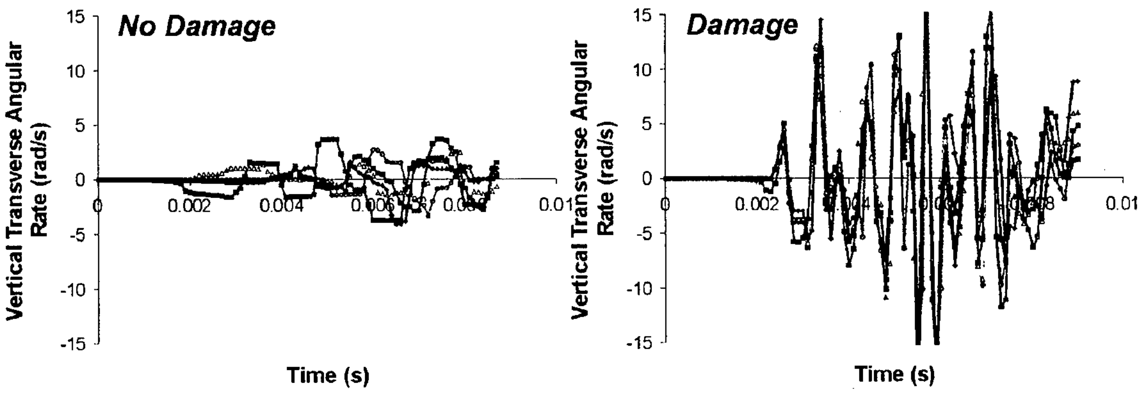

FIGURE 19. VARIABILITY VS. PRESSURE PULSE SIZE AND LOCATION.

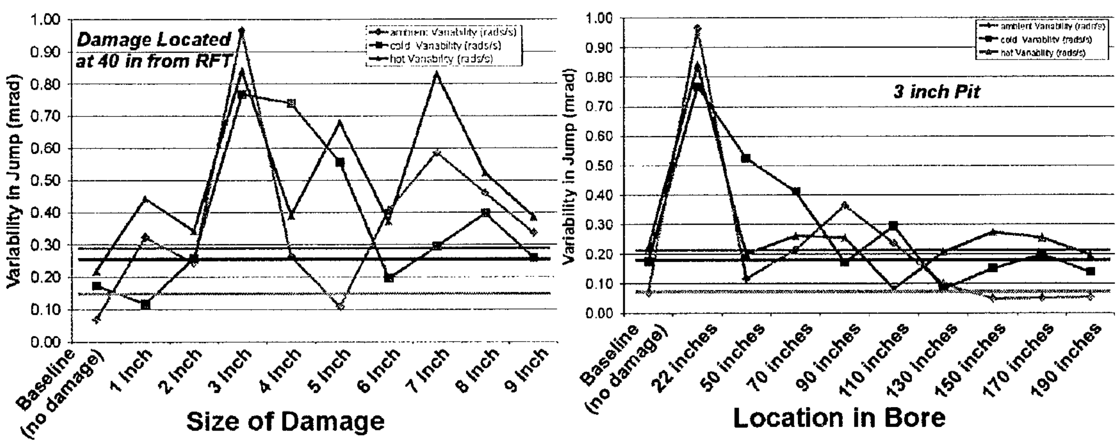

FIGURE 20. MUZZLE JUMP VARIABILITY VERSUS PRESSURE PULSE SIZE AND LOCATION.

8.0 HYPOTHESIS FOR OCCASIONAL ERRATIC BEHAVIOR

Occasionally, erratic flight behavior of the M831A1 has been observed. The behavior typically manifests itself as a target impact that is significantly out of pattern or by a ground impact short of the target. There are currently at least five theories that provide potential explanations for this behavior: (1) poor launch dynamics, (2) roll-yaw lock-in, (3) aerodynamic trim-induced trajectory bias (4) discarding obturator, and (5) sealing ring interference with the stabilizer. The occurrence of occasional high yaw rates was demonstrated at TEF (Soencksen, Newill, Plostins, 2000). While these theories are documented here, the source of the theories is referenced.

The first hypothesis is the result of the study presented in this paper. If a gun tube has bore damage , and if the obturator system is not able to prevent local jetting, then the dynamic path of the projectile can be altered. The second theory is that roll-yaw lock-in, (Arrowtech Associates Inc and Alliant, 1999) is related to the very slow roll-up of the projectile observed in experiments. Since the projectile is full-bore and heavy, it has a large axial moment of inertia. These attributes, coupled with the fact that the stabilizer diameter is smaller than the body diameter, and implies that the stabilizer is not wetted by the free stream sufficiently. This limits available roll torque. The low torque available combined with the high axial moment of inertia results in the very slow projectile roll up . This was shown experimentally by Soencksen, et al. (2001). Since the projectile is slowly rolling, as the roll frequency approaches the yaw frequency, resonance can occasionally cause catastrophic yaw amplification, which leads to drastically increased drag, and thus a potential short ground impact. The slow roll characteristics may also be responsible for trajectory bias in the event that aerodynamic trims are present. Such trims were shown in TEF experimental data (Soencksen, et. al, 2000), and a detailed description of their effect on the trajectory is found in that work. The forth theory is related to discard of the obturator band, which occurs approximately 50% of the time. Occasionally, as the band attempts to discard, it either gets temporarily caught on the obturator seat or becomes stuck in the seat (Manole, 1998). If this occurs such that the band stays partially attached to the projectile throughout the flight, this could adversely affect the flight in two ways. First, the hanging band will create an asymmetry that will lead to a trim and potentially a trim-induced trajectory bias. Secondly, drag could also be affected. The final theory was also observed during ballistic testing by Alliant Techsystems (Demitroff 2000). During the test, Hadland digital photographs show a projectile where the sealing ring did not break or discard at muzzle-exit as is normally the case. In this case, the ring slipped over the retaining ring, moving aft and seating at the end of the stabilizer (Figure 21), partially masking the slots used to generate roll torque.

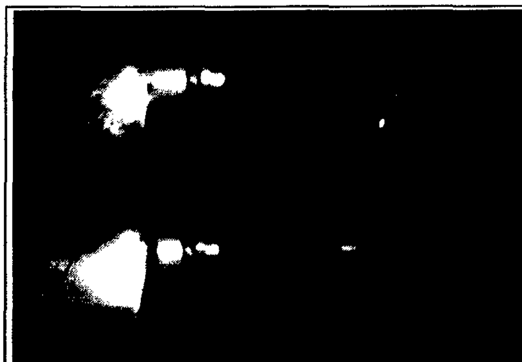

Launch with Sealing Ring on Back of Stabilizer

FIGURE 21. NORMAL LAUNCH AND SEALING RING ON THE STABILIZER.

Its final observed position during flight was on the back of the stabilizer covering the slots used to generate spin-up torque. If the ring stays in this position throughout the flight, it could adversely affect roll torque generation, possibly causing changes in the jump.

9.0 CONCLUSION

This paper analyzes the launch dynamics of the M831A1 using computer simulation technology, and validating the simulations with experimental data. The launch cycle and its effects on the M831A1 are described showing that the projectile spends a relatively long period of time in the bore of the gun. Even

with the long dwell times, the launch dynamics of the projectile are similar to those of a typical prototype kinetic energy (KE) projectile. This does not imply that the launch of the projectile occurs without disturbance. While the initial effects on the projectile are symmetric, as the launch cycle proceeds, the projectile exhibits balloting behavior leading to asymmetric effects. While not as severe as the balloting seen for the M865, the balloting is still violent enough to cause flexing in the steel nose spike during launch. While the balloting behavior contributes some of the variability at muzzle-exit, the gun tube shape remains one of the dominant influences. Overall, the projectile performance is good provided it is manufactured within specified tolerances and is not subjected to large lateral forces from bore erosion. When bore erosion is present, it has the largest influence in the early portion of the launch cycle since it has a longer action time due to the projectile's relatively low velocity here. Bore erosion affects obturation of the propellant gases. Simulations show that while the current obturation system appears adequate, there are some questionable aspects of its behavior. Simulations suggest a remedy to address the issue and is scheduled for ballistic testing. Finally, the simulations have been compared to experimental data obtained at TEF with good agreement. The ultimate result of this work has been a better understanding of the launch dynamic effects on the projectile, and to offer explanations for the occasional erratic ballistic behavior.

10.0 ACKNOWLEDGEMENT

A study of this magnitude requires a coordinated effort and support from many people. The principal organizations are ARL, ARDEC's AMSTA-AR-CCH-B, Rock Island Operations Support Command, Alliant Techsystem Inc, General Dynamics Ordnance and Tactical Systems, and the people at ARL. Their leadership expertise and experience are invaluable. This study relied heavily on supercomputers supplied by DOD's High Performance Computing initiative (specifically by the Major Shared Resource Center at ARL).

11.0 REFERENCES

Anderson, R. D., and K. D. Fickie. "IBHVG2 - A User's Guide." BRL-TR-2829, APG, MD, Jul 1987.

Bornstein, J., I. Celmins, and P. Plostins, "Launch Dynamics of Fin-Stabilized Projectiles." AIAA Paper No. 89-3395, Aug 1989.

Bornstein, J., I. Celmins, P. Plostins, E. M. Schmidt. "Techniques for the Measurement of Tank Cannon Jump." BRL-MR-3715, U.S. Army Ballistic Research Laboratory, Aberdeen Proving Ground, MD, Dec 1988.

Bundy M. L., J. F. Newill, and C. P. R. Hoppel, "A Notional Redesign of the M865E3 Obt." ARL-TR-2325, Sep 00.

Bundy M., J. Newill, V. Marcopoli, M. Ng, C. Wells, "A Meth. for Char. Barrel Flex. Due to Tank Motion." ARL-MR-479, Jun 00

Burns B. P. , D. L. Henry, C. D. McCall, J. F. Newill, "Flex. Char. of the M829 Proj. Family." ARL-TR-1201, Sep 96.

Burns B. P. , J. F. Newill, and S. A. Wilkerson, "In-Bore Projectile Gun Dynamics." *Proceedings of the 17th International Ballistics Symposium*, Midran, South Africa, 26 Mar 98.

Cote, P.J., Rickard, C., " Gas Metal Reaction Prod. in the Erosion of Chromium Pltd Gun Bores" Wear, Vol. 241, Is. 1 pp 17-25, Jun 00.

Demitroff, D., Personal communication with J. Newill. Alliant Techsystems, Hopkins, MN, 1998-2000.

Dohrn, R. Personal communication J. Newill. Alliant Techsystems, Hopkins, MN, 1998-2000.

Guidos B. , P. Plostins, D. Webb, J. F. Newill, "120-mm Tank Gun Acc. Demonstrator (TGAD) Jump Test." ARL-TR-29, Dec 99.

Gazonas, G.A., "Impl. Of A Finite Strain Plasticity Model For Nylon 6/6 Into DYNA3D", in: *Structures Under Shock and Impact VI*: N. Jones, C.A. Brebbia, and A.J. Watson [Editors], Comp. Mech. Pub., Ashurst Lodge, Ashurst, Southhampton, UK, Jul 00.

Hoppel C.P.R., J. F. Newill, and K. P. Soencksen, "Evaluation of Obturator and Sealing Cuff Properties for the M865 Training Projectile with Comparison to Ballistic Testing." ARL-TR-2039, APG, MD, Sep 99.

Lyon, D. H. "Radial Stiffness Measurements of 120-mm Tank Projectiles." ARL-TR-392, U.S. Army Research Laboratory, Aberdeen Proving Ground, MD, Apr 94.

Lyon, D. H. and K. P. Soencksen. "Radial Stiffness and In-Bore Balloting Analysis for the M900 Projectile." ARL-TR-593, U.S. Army Research Laboratory, Aberdeen Proving Ground, MD, Oct 94.

Manole L., Personal communication with J. Newill. ARDEC, Picatinny Arsenal NJ, 1998-2000.

Newill J. F., B. P. Burns, and S. A. Wilkerson, "Overview of Gun Dynamics Numerical Sim." ARL-TR-1760, APG, MD, Sep 98a.

Newill J. F., C. P. R. Hoppel, D. Kamdar, B. Guidos, and B. Drysdale, C. Livecchia, and M. Luciano, "Geometric and Material Changes to the Forward Bourrelet to Optimize Performance of KE Ammunition." ARL-TR-2328, Sept 00.

Newill J. F., C. P. R. Hoppel, K. P. Soencksen, and P. Plostins, "Simulation of the M865 Kinetic Energy Projectile with Experimental Validation." Proceedings of the 18th International Ballistics Symposium, San Antonio, TX, Nov 99a.

Newill J. F., C. P. R. Hoppel, W. H. Drysdale, and D. S. Kamdar, "Effects of Bourrelet Stiffness on the Interior Ballistic Performance of Kinetic Energy Ammunition." ARL-TR-02, APG, MD, Jun 99b.

Newill J. F., C. P. R. Hoppel, W. H. Drysdale, and S. A. Wilkerson "Numerical Simulation of Launch Interaction of Kinetic Energy Long Rod Fin-Stabilized Projectiles and M1A1 Abrams M256 Gun System with Comparison to Experimental Results." National Def. Industrial Assoc. 48th Annual Bomb & Warhead Technical Symp., Eglin Air Force Base, FL. May 11-14, 98b.

Newill J. F., C. P. R. Hoppel, and W. H. Drysdale, "Comp. of Launch Mechanics and Dynamics from the M1A1 M256 Gun System for the M829A2 Kinetic Energy Long Rod Fin Stabilized Projectile Containing Diff. Penetrator Materials." ARL-TR- 1671, . Apr 98c.

Newill J. F., S. A. Wilkerson, C. P. R. Hoppel, and W. H. Drysdale. "Numerical Simulation of Composite Kinetic Energy Projectiles Launched by an M1A1 Abrams M256 Gun System." Proc. of the 30th SAMPE Technical Conference, San Antonio, TX, 23 Oct 98d

Newill, J. F., D. Webb, B. Guidos, C. P. R. Hoppel, and W. H. Drysdale. "Meth.. for Formal Comp. of Exp. Ballistic Firing of Kinetic Energy Projectiles With Num. Sim." Technical Report, U.S. Army Research Laboratory, APG, MD, in progress.

Plostins, P., I. Celmins, and J. Bornstein. "The Effect of Sabot Front Borerider Stiffness on the Launch Dynamics of Fin-Stabilized Kinetic Energy Ammunition." AIAA Paper No. 90-0066, Jan 90.

Rabern D.A., "Axially Acc. Saboted Rods Subjected to Lateral Forces." BRL Contractor Report No. 671, Aug 91.

Schmidt, E. M., P. Plostins, and M. Bundy. "Flash Radiographic Diagnostics of Proj. Launch from Cannon." Proc. of Flash Radiography Symposium, E.A. Webster, Jr. and A.M. Kennedy, editors., The American Society for Nondestructive Testing, 84.

Soencksen K.P., J. F. Newill, P. Plostins, "Aerodynamics of the 120-mm M831A1 Projectile: Analysis of Free-Flight Experimental Data." Proceedings of AIAA Atmospheric Flight Mechanics Conference & Exhibit, Denver, AIAA-00-4198, CO, 14-17 Aug, 00

Soencksen, K. P., J. F. Newill, J. M. Garner, and P. Plostins, "Comp. of the 120-mm M831A1 Projectile's Exp. Launch Dynamic Data with Hydrocode Gun-Projectile Dynamic Simulations." 10th Army Gun Dynamics Symposium, Austin, TX, 23 – 26 Apr 01

Soencksen, K.P., J.F. Newill, P. Plostins, "Roll Characteristics of the 120-mm M831A1 Projectile." *Proceedings of the 39th AIAA Aerospace Sciences Meeting & Exhibit,* 8-11 January 2001, Reno, NV.

Whirley R. G, D. E. Englemann, and J. O. Hallquist. "DYNA3D; A Nonlinear, Explicit, 3-D Finite Element Code for Solid and Structural Mechanics - User's Manual" Lawrence Livermore's National Laboratory, UCRL-MA-107254 Rev 1, Nov 93.

Wilkerson S. A. and D. Hopkins, "Analysis of a Balanced Breech System for the M1A1 Main Gun System Using Finite Element Techniques." Army Research Laboratory Technical Report 608, Nov 94.